Supplementary Information (SI) for Journal of Materials Chemistry C.

Supporting Information

Morphological Optimization of Au Nanostars (AuNS)

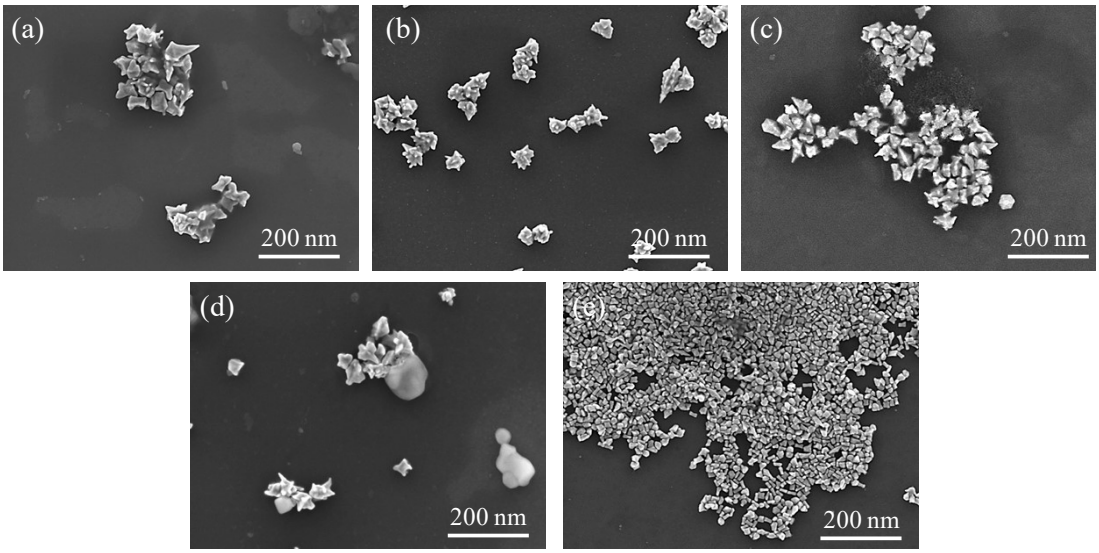

Fig. S1. SEM of AuNS prepared with different volumes of 0.01 M $AgNO_3$ (a) 138 µL; (b) 168 µL; (c) 198 µL; (d) 228 µL; and (e) 258 µL.

Gold seeds were prepared by reducing Au^{3+} in chloroauric acid using sodium borohydride ($NaBH_4$). Subsequently, the gold seeds were grown in a solution containing ascorbic acid as a reducing agent and Ag^+ ions, resulting in the formation of gold nanostars (AuNS). AuNS of different particle sizes can be obtained by changing the content of silver nitrate. As shown in Figures S1(a)-S1(e), AuNS were synthesized with 138, 168, 198, 228, and 258 µL of $AgNO_3$ solution. The average particle diameter decreased with increasing $AgNO_3$ content. With addition of 198 µL, the AuNS exhibited uniform branching, good dispersion, and optimal morphology. When the added volume exceeded 198 µL, the resulting nanostructures gradually transformed into smaller particles with irregular shapes and increased aggregation. The average size of AuNS decreased significantly with increasing Ag^+ content, indicating that Ag^+ plays a crucial role in determining their morphology.

AuNSs SERS Performance for R6G Detection

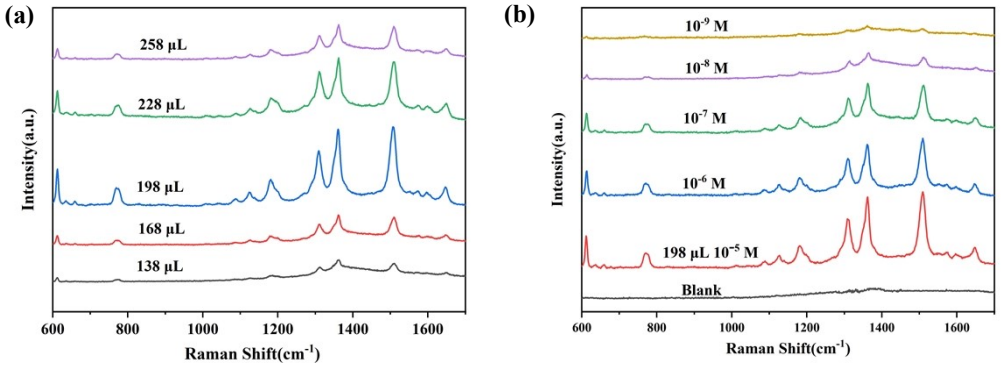

Fig. S2. (a) SERS spectra of R6G (10^{-5} M) with AuNS substrates fabricated with varying volumes of 0.01M $AgNO_3$; (b) SERS detection limit spectra of R6G probe with AuNS substrates prepared using 198 µL $AgNO_3$.

Figure S2 (a) presents the SERS spectra of 10^{-5} M R6G obtained using AuNS substrates prepared with different volumes of 0.01M $AgNO_3$. The SERS signal intensity initially increased and then decreased with increasing addition of Ag^+, reaching its maximum at 198 μL. Applying this optimized condition, Figure S2(b) presents the detection sensitivity of the substrate towards R6G. As the concentration of R6G decreased from 10^{-5} M to 10^{-9} M, the intensity of the characteristic Raman signals successively diminished. At 10^{-9} M, the SERS signals became barely distinguishable, indicating the LOD.

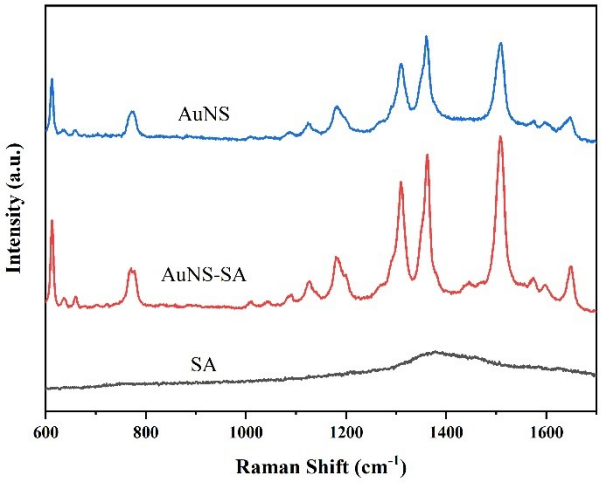

Fig S3 Detection of the SERS spectra of 10^{-5} M R6G using different materials as the substrate.

As shown in Figure S3, the SERS spectra of R6G at a concentration of 10^{-5} M were compared using three different substrates: AuNS, AuNS-SA, and SA. It can be observed that the composite material AuNS-SA exhibits the strongest Raman enhancement, followed by AuNS alone. In contrast, the silica aerogel (SA) substrate shows almost no characteristic peaks for R6G.

BET Tests for AuNS and AuNS-SA

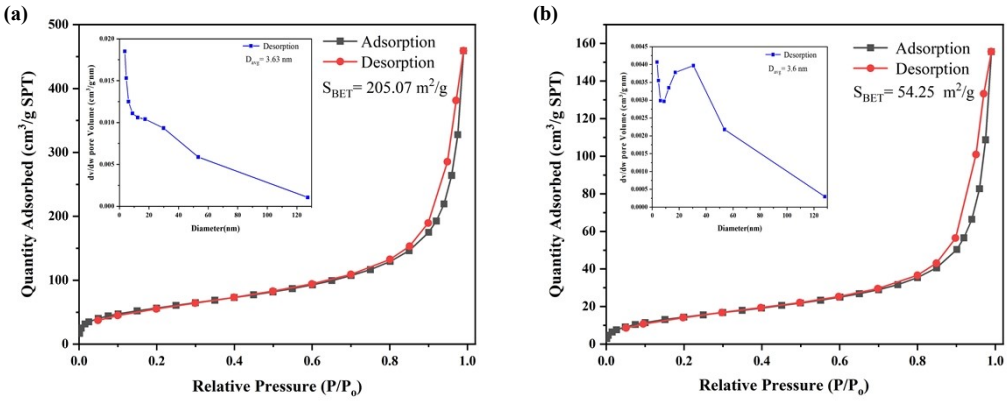

Fig S4. Nitrogen adsorption-desorption isotherms of (a) Silica Aerogel (b) AuNS-SA; Inset: corresponding pore size distribution.

BET testing was performed using an American Quantachrome ASiQwin instrument. Nitrogen adsorption-desorption measurements were conducted on the samples at 77.35 K under liquid

nitrogen conditions. As shown in the Fig S4, the specific surface area of the silica aerogel was 205.07 m^2/g, while that of the AuNS-SA composite was 54.25 m^2/g. The significant decrease in specific surface area after compositing is likely attributed to the loading of AuNS onto the pore channels or surface of the aerogel, which occupied part of the pore space.

AuNS Thermogravimetric Analysis (TGA)

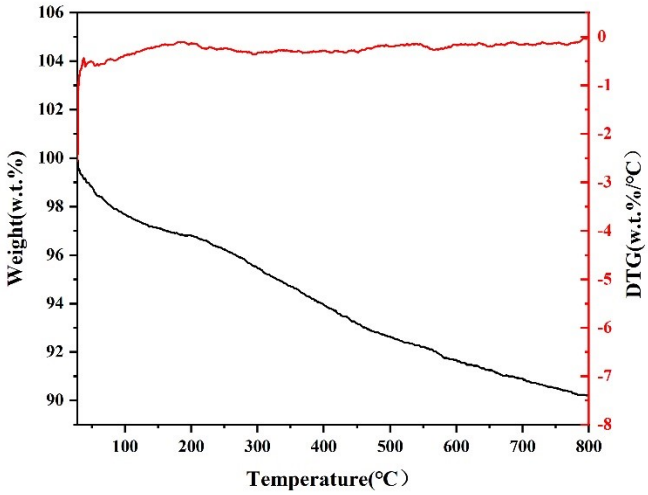

Fig S5. TG-DTA curves of the AuNS-SA composite.

To investigate whether the AuNS-SA composite achieves firm immobilization, thermogravimetric-differential thermal analysis (TG-DTA) was performed using a German NETZSCH STA 449 F3 thermal analyzer. The results are shown in the Fig S5. The analysis was conducted under a nitrogen atmosphere with a heating rate of 20 °C/min over a temperature range from 28 °C to 800 °C. The AuNS-SA composite exhibited a relatively small total weight loss, and no distinct weight loss plateau was observed on the thermogravimetric curve. This result reflects, on the one hand, the excellent thermal stability of the silica aerogel framework itself, and on the other hand, indirectly suggests that a relatively stable binding state is formed between the gold nanostars and the aerogel, preventing significant mass changes caused by interfacial desorption or aggregation during the heating process.

SERS Performance Factor (SPF) estimation

Referring to the article by Yue et al. (2024) published in Analytical Chemistry (96: 17517-17525), which discusses the SERS performance factor as a standardized evaluation parameter.

$$\mathrm{SPF} = \frac{\Delta I_{\mathrm{SERS}}}{\Delta C_{\mathrm{SRES}}} \Big/ \frac{\Delta I_{\mathrm{Raman}}}{\Delta C_{\mathrm{Raman}}}$$

SPF stands for SERS performance factor. Under the same or standardized measurement conditions, it is calculated as the ratio of the slope of the concentration-dependent SERS intensity response (below monolayer coverage) to that of the conventional Raman intensity response within the linear dynamic range (i.e., sensitivity).

From the figure, it can be seen that the SERS slope is 257.73 and the Raman slope is 88.30. Concentration is 10^{-9} M~10^{-14} M, Substituting these values into the formula:

$$SPF = \frac{\Delta I_{SERS}}{\Delta C_{SRES}} \Big/ \frac{\Delta I_{Raman}}{\Delta C_{Raman}} = 2.92 \times 10^5$$

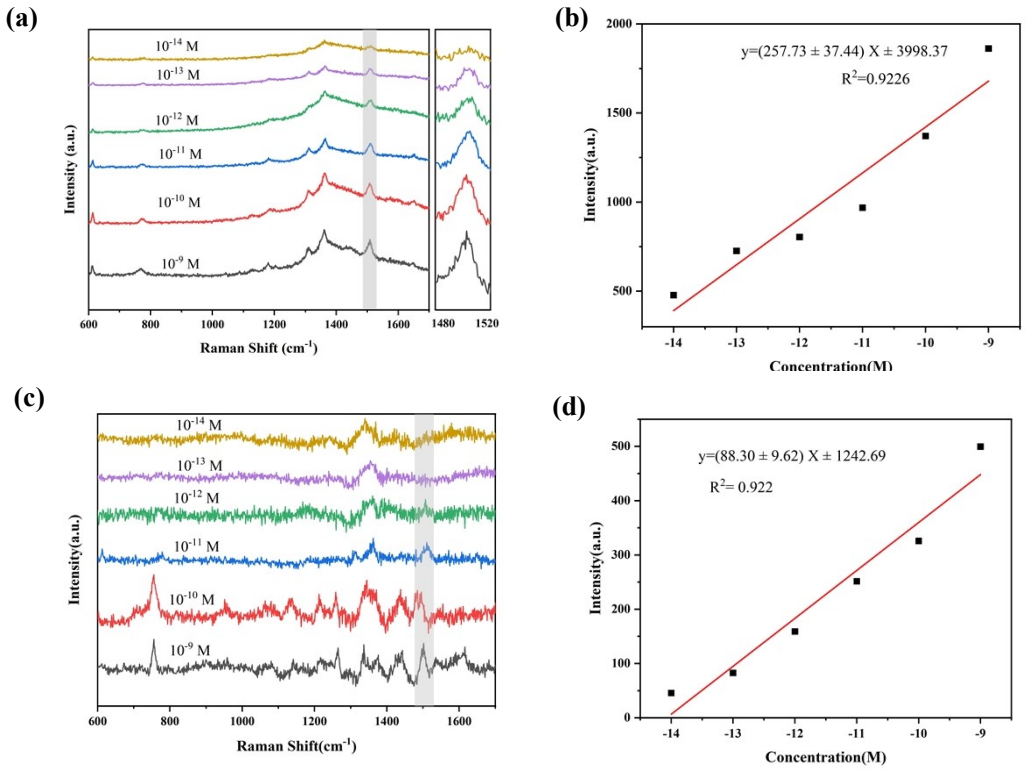

Fig.S6. (a) R6G concentration dependent SERS spectra; (b) SERS intensity at 1507 cm^{-1}; (c) R6G concentration dependent normal Raman spectra; (d) Raman intensity at 1507 cm^{-1}.